


Article

Anisotropy and Fiber Orientation: A Key Player in the Lateral Imbibition of Cellulose Paper

Pierre-Yves Bloch ^{1,*}, Jean-François Bloch ^{1,2}, Konrad Olejnik ³  and Daniel Brissaud ¹

¹ 3SR and G-SCOP, University Grenoble Alpes, CNRS, 38000 Grenoble, France; jean-francois.bloch@grenoble-inp.fr (J.-F.B.)

² BeFC SAS, 31 Rue Gustave Eiffel, 38000 Grenoble, France

³ Centre of Papermaking and Printing, Lodz University of Technology, 93-005 Lodz, Poland; konrad.olejnik@p.lodz.pl

* Correspondence: pierre-yves.bloch@grenoble-inp.fr; Tel.: +33-(0)-6-67-21-05-66

Abstract: In this article, we delve into the influence of fiber orientation (structural anisotropy) on paper imbibition, with a particular focus on in-plane imbibition. Utilizing the XLPA experimental method, we analyze several papers with different anisotropies, employing a constant volume of ethanol as the imbibing fluid. Our findings contribute novel insights into the anisotropic behavior of imbibition, a topic not extensively covered in the literature. We analyze how the orientation of fibers significantly influences lateral imbibition, providing a deeper understanding of the microfluidic properties of paper. The anisotropies found for imbibition fit perfectly with the existing data found in the literature, indicating the influence of fiber orientation. Furthermore, the kinetics are shown to be linked directly with the porosity.

Keywords: fiber orientation; anisotropy; imbibition; physical properties



Citation: Bloch, P.-Y.; Bloch, J.-F.; Olejnik, K.; Brissaud, D. Anisotropy and Fiber Orientation: A Key Player in the Lateral Imbibition of Cellulose Paper. *Fibers* **2024**, *12*, 56. <https://doi.org/10.3390/fib12070056>

Academic Editor: Martin J. D. Clift

Received: 23 April 2024

Revised: 20 June 2024

Accepted: 26 June 2024

Published: 3 July 2024



Copyright: © 2024 by the authors. Licensee MDPI, Basel, Switzerland. This article is an open access article distributed under the terms and conditions of the Creative Commons Attribution (CC BY) license (<https://creativecommons.org/licenses/by/4.0/>).

1. Introduction

Lignocellulosic fibers used in paper production have a complex, multi-layered physical and chemical structure, which is additionally modified during the process of preparing the fibrous raw material for paper production. The spatial organization of the cellulose fiber, especially the way it is located (oriented and aggregated) in the paper structure and bonded to other fibers, determines the physical properties of this material [1,2].

During the web formation, the most important factor consists of the difference between the velocities of the pulp jet and the wire. Indeed, the difference in velocities initiates a shear stress acting on the fiber aggregates in the pulp [3], which is responsible for the alignment of the fibers, mainly in the machine direction. Note that thickness is also important as a thin jet will lead to higher shear and, therefore, higher orientation than a thick jet. The distribution of fiber orientation is consequently modified by a change in the difference between the jet and wire velocities.

In forming a paper web, the fibers are aligned predominantly in the same plane; however, they are not aligned equally in all directions. Statistically (Figure 1), more fibers are aligned parallel to the movement of the formed paper web (Machine Direction—MD), and fewer are aligned across the machine direction (CD—Cross Direction) [3,4].

The fiber orientation must be considered in both the in-plane and out-of-plane directions. For the latter, the fiber angle is less than 5°. Hence, paper is often considered as a layered structure (Figure 2).

A fiber orientation index and an angle may be used to characterize the in-plane distribution. The angle indicates the misalignment of the main fiber orientation with the machine direction due to hydrodynamics effects. Note that this angle is different from the mean angle, which may reach 65° for highly oriented papers (CD as a reference for the angle) and is equal to 45° for isotropic paper.

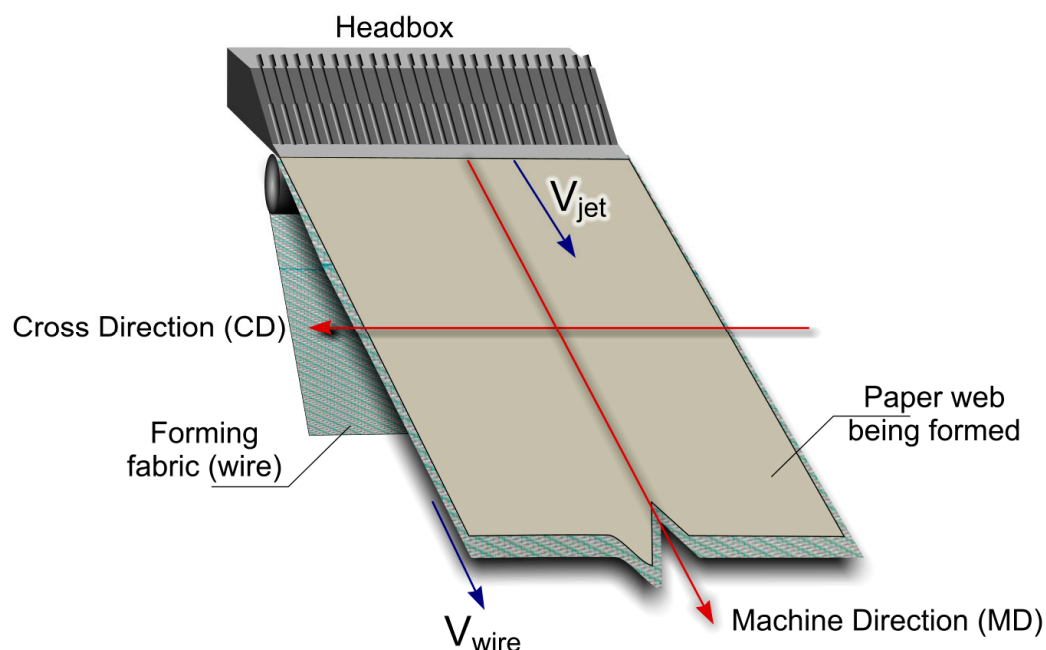


Figure 1. Scheme of forming a paper web on a paper machine wire. The main directions and velocities are indicated.

The fiber orientation affects, in particular, the in-plane mechanical properties of paper, such as the Young modulus, tensile index, elongation, tear strength, stiffness, as well as dimensional stability [5].

Several experimental techniques are used to obtain the distribution of the fibers' orientation in a paper web, such as presented in Yang [6] or in Fiadero [7]. In particular, direct or indirect methods are used [4] as described, for example, in Dias [8]. Then, a mathematical description is required to characterize the distribution. For example, in 1971, Wahren [9] introduced for example a distribution in terms of the development of Fourier, here restricted to cosines in the first order (Equation (1)):

$$f(\alpha) = \frac{1}{2\pi}(1 + e \cdot \cos 2\alpha) \quad (1)$$

where α represents the fiber angle and $\alpha = 0$ is the machine direction.

Here, the parameter, e , describes the anisotropy in this model.

Fiber orientation is, hence, often introduced in such distributions as an anisotropy factor, such as q in the example of Niskanen [5] presented in Figure 2. This anisotropy is here only related to the geometry or structure.

Paper materials have a capillary-porous structure. This structure and its properties originate from the way the fibers are arranged and distributed in it [10]. Thanks to hydrophilic cellulose fibers, the paper structure has good liquid transportation and absorption properties. The anisotropy of paper structure also affects liquid absorbency [11,12]. The absorbent properties of paper are essential in many different applications (e.g., printing processes, packaging production, hygiene materials, microfluidic paper-based devices, etc.), which is why research on this issue is still the focus of interest of many scientists [13–17].

The aim of this study was to analyze the relationship between structural anisotropy and other physical properties, such as porosity or permeability, focusing on in-plane imbibition. In particular, this research aimed to answer the question: does geometric anisotropy influence the imbibition anisotropy?

In the presented research, we will focus only on the geometrical aspects, as we will only consider different fiber orientations.

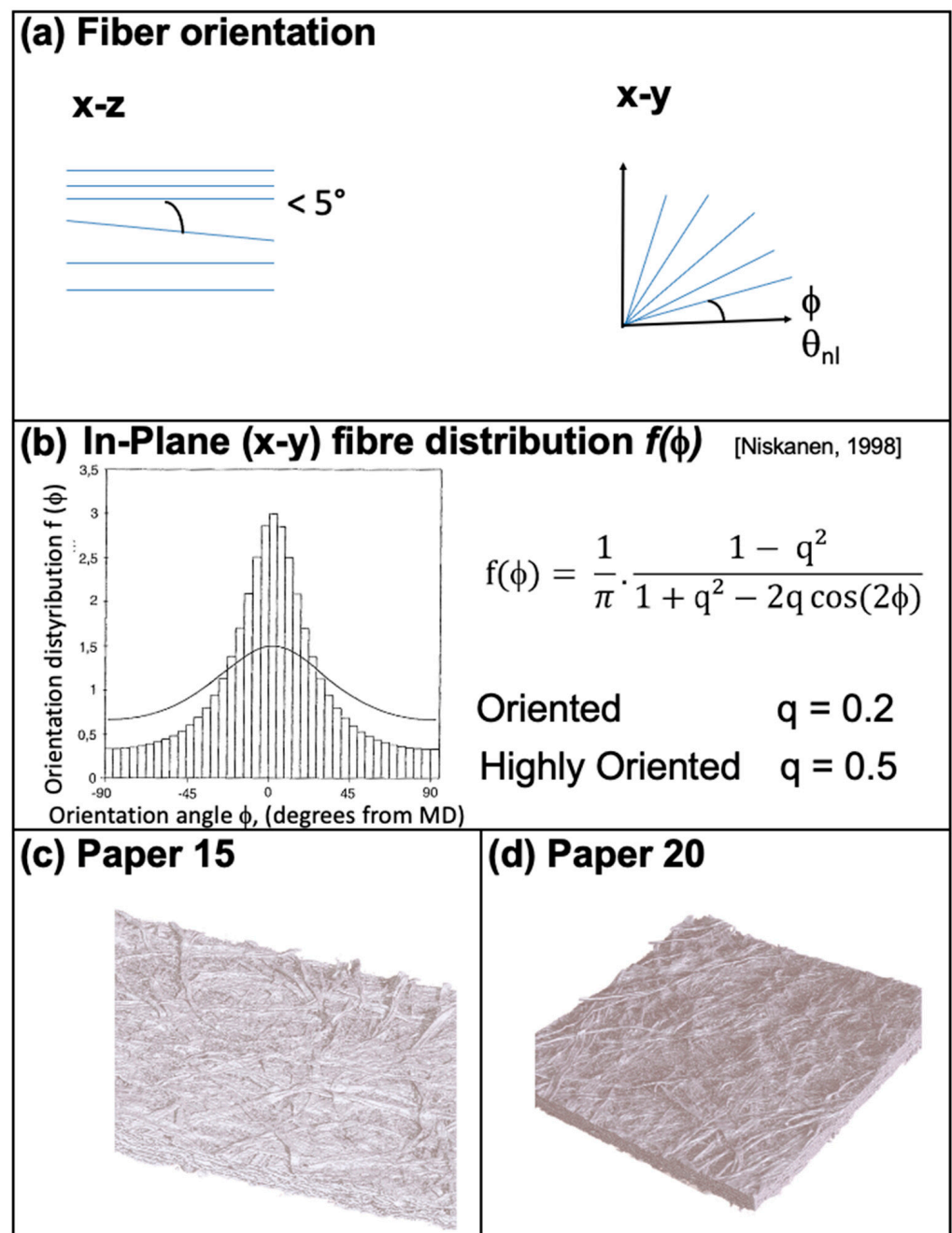


Figure 2. Fiber orientation: (a) thickness x-z and in-plane x-y directions (schematic), (b) in-plane distribution of fiber orientation f ([2]), and (c,d) X-ray microtomography for papers referenced as 15 and 20, respectively. The papers are presented in the materials and methods section.

2. Materials and Methods

2.1. Materials

Ethanol was chosen as (i) it passes quickly through the studied papers and (ii) it creates a visual contrast, allowing image analysis. Ethanol (96%, AR quality) was acquired from CHEMPUR Company, Piekary Slaskie, Poland.

Paper samples with known anisotropy were used in the presented studies. The difference between the velocity of the jet and the wire was used as a coefficient characterizing the anisotropy.

The distribution of fiber orientation is modified by changes in the difference between the jet and wire velocities, as illustrated in Table 1.

Table 1. Influence of jet and wire velocities on fiber orientation and main physical properties for the different reference papers (labeled 15 to 20).

Paper Samples Data from the Literature	18	19	20	16	15
$V_{\text{jet}} - V_{\text{wire}} \text{ (m}\cdot\text{min}^{-1}\text{)}$	−29.5	−17.4	−5.7	8.6	29.8
θ_{nl}	61.5	56.1	48.7	55.9	60
a/b colorimetric	1.97	1.42	1.13	1.41	1.71
$W \text{ (g}\cdot\text{m}^{-2}\text{)}$	50.9	48.6	48.5	48.2	47.7
e (μm)	86	82	90	87	89
Porosity	0.615	0.615	0.650	0.640	0.652
Young Modulus ($\text{kN}\cdot\text{cm}^{-2}$)					
MD	532	434	317	378	466
CD	114	152	150	113	111
Mean	323	293	235	264	288
MD/CD	4.7	2.8	2.1	3.3	4.2

A few distribution functions exist in the literature, such as the von Mises one or Fourier series, which can be used to characterize the fiber orientation in a paper structure. An example is presented in Figure 2b. Note that the mean angle may be used as a single parameter to describe the distribution of fiber orientation. The drawback of this simple parameter is that there is no unique relation between a mean angle and the distribution.

In the present study, dyed fibers were incorporated into the paper used to facilitate the orientation characterization. The set of papers referenced as 15, 16, 18–20 are pilot-plant papers manufactured at a rate of $80 \text{ m}\cdot\text{min}^{-1}$ by the Pagora/Grenoble INP (known also as École Française de Papeterie et des Industries Graphiques de Grenoble (EFG)). These paper samples are 100% kraft-bleached softwood pulp, beaten to 430 CSF (SR-30). The fiber's composition, and, in particular, the lignin/cellulose ratio, influences the web formation [18]. As only one type of fiber is used here, this parameter is not included in our discussion.

Hence, for decades, this method has been used intensively to characterize the influence of the difference in velocities on fiber orientation, and then on paper properties. We used these samples as many data are available in the literature. Indeed, they have been used to validate the experimental technique. An example of the validation of such a technique and the use of these papers is (Fiadero, 2002) [7], involving a diffraction technique to characterize fiber orientation. For the purpose of this research, we also extracted data from the literature [16].

We have included the mean θ_{nl} weighted by the length of fibers. We note that the mean angles θ vary as expected from 48.7 (close to 45, which corresponds to an isotropic sheet) to 61.5. We also introduced here an ellipticity (a/b) obtained from the direct measurement of the orientation of the dyed fibers. The interested reader may refer to the following literature [3,19–22].

The difference between the wire and the jet velocities influences, on the one hand, fiber orientation and, on the other hand, the physical properties, as exemplified in Figure 3.

It is clearly visible that the fiber orientation is influenced by the difference in the V_{jet} and V_{wire} velocities. Furthermore, the anisotropy of the Young modulus is proportional to the fiber orientation. The same tendency can be found in the literature (Figure 2c). A biunivoque relation between these anisotropies does, however, not exist, as drying conditions, for example, may affect the mechanical anisotropy. Permeability is also influenced by fiber orientation (Appendix A). In this case, the higher value corresponds to the isotropic case, as illustrated in Figure 2d. We analyze hereafter the anisotropic behavior as well as the kinetics of imbibition.

Ethanol at a temperature of $22 \text{ }^\circ\text{C}$ was used for the tests.

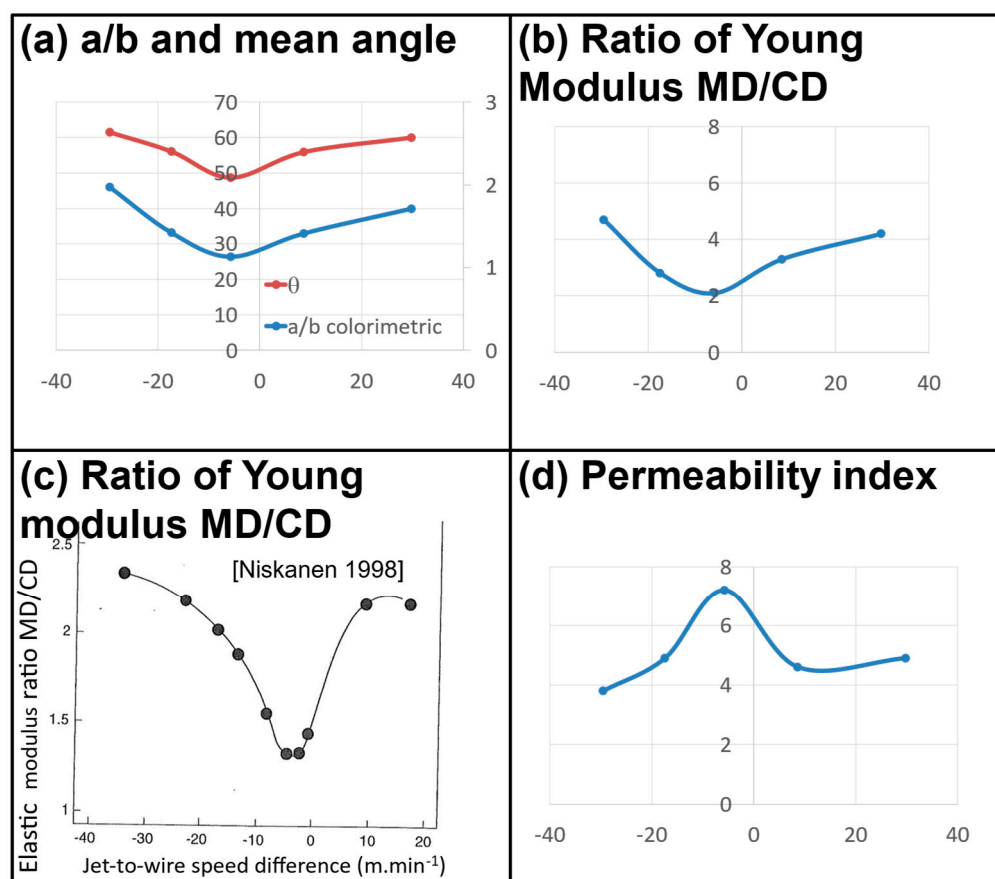


Figure 3. Physical properties vs. difference in jet to wire velocities (a) a/b and mean angle, (b) Ratio of Young Modulus, (c) Ratio of Young Modulus, data from Niskanen [2], and (d) permeability index. The studied papers (15–20) are used in (a,b,d). The results in (c) are taken from Niskanen for other papers at machine speed 450 m·min⁻¹.

2.2. Methods

The experiments were performed with the eXtended Liquid Penetration Analyser (XLPA) as described by [23]. The XLPA is a device that enables the visual analysis of the geometric evolution of the spot formed by the diffusion of a liquid in a substrate, as shown in Figure 4.

Bendtsen air permeability [24] was used as the method to evaluate the influence of fiber orientation on the average porosity of paper samples.

Paper thickness was measured on a Lhomargy micrometer ([25]).

Porosity P was calculated from the thickness and basis weight as follows (Equation (2)):

$$P = 1 - \frac{W}{t \cdot \rho_0} \quad (2)$$

where P , W , t , and ρ_0 represent the porosity, basis weight, thickness, and density of cellulose (1540 kg·m⁻³), respectively.

The Lippke method was also used to characterize the anisotropy of paper, which consists of the transmission of a circular laser beam (near-infrared laser) through the thickness of paper by normal incidence. The ellipsoid shape obtained due to the distribution of fibers is then analyzed in terms of ellipticity [26].

Another experimental method is based on the analysis of laser diffraction patterns produced by transparent replicas of the fiber web surfaces. The diffraction method uses a polymer replica and then a laser transmission analysis, using a plane-parallel beam of laser light to illuminate a transparent surface replica. The 2D Fourier transformation of

the paper replica is an elliptical shape with a specific ellipticity ratio [7]. The colorimetric method uses colored fibers and then analyzes transmitted images.

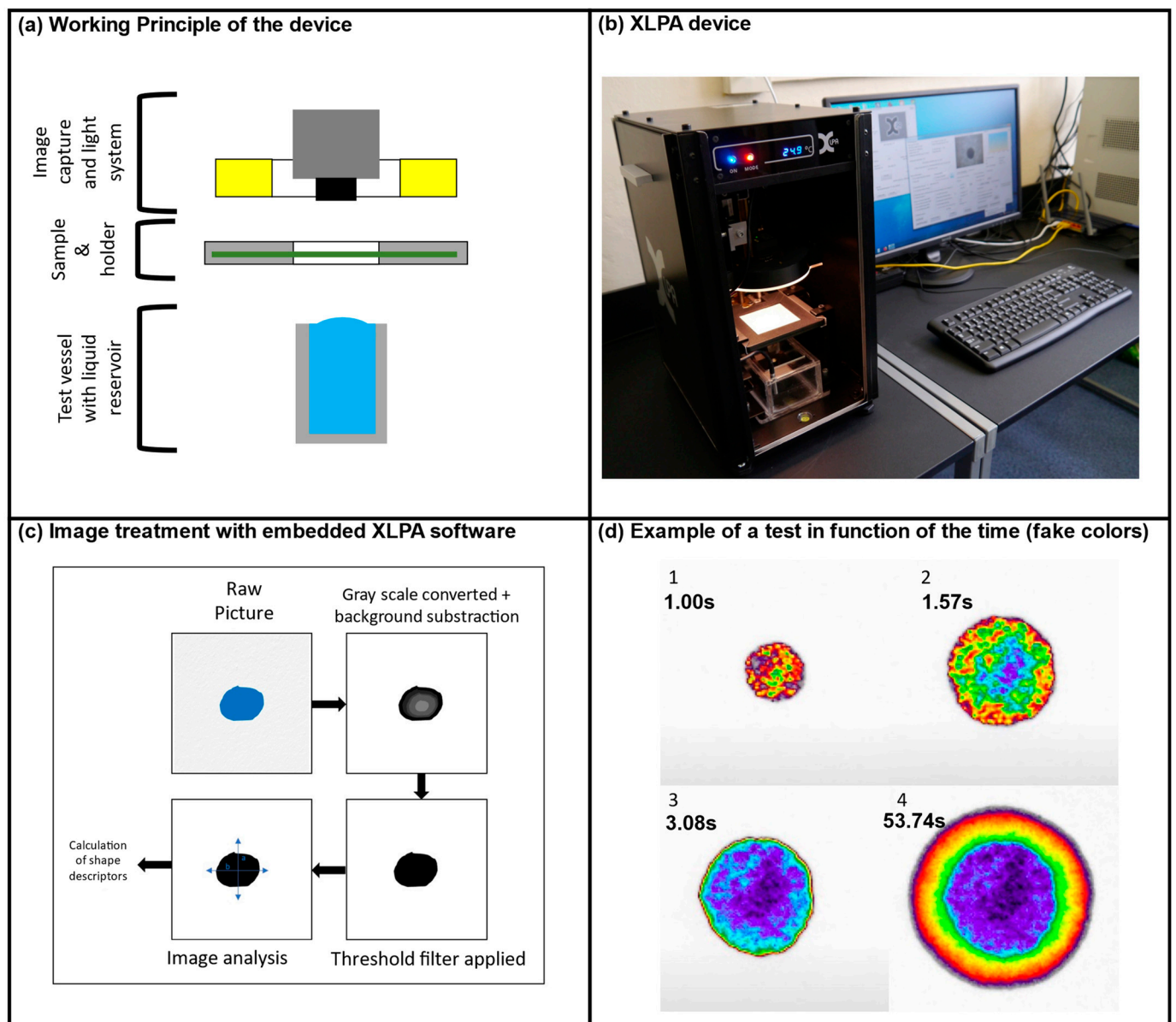


Figure 4. XLPA device with (a) working principle of the device, (b) XLPA device, (c) image treatment with embedded XLPA software (version 1.0), and (d) example of a test in function of the time.

3. Results

The first results concern the overall liquid imbibition of the tested samples. We consider here both the anisotropy and its evolution, and both the major and minor axes of the observed ellipse. It must be emphasized that the spread of liquids in the heterogeneous structure of paper is very difficult to analyze. As a result, the properties of this material may vary even when samples are taken from the same paper roll. During the presented tests, the measurements were repeated at least five times for each paper, and the curves that were repeatable were selected for analysis. The results of the imbibition kinetics for paper samples of different anisotropies are presented in Figure 5.

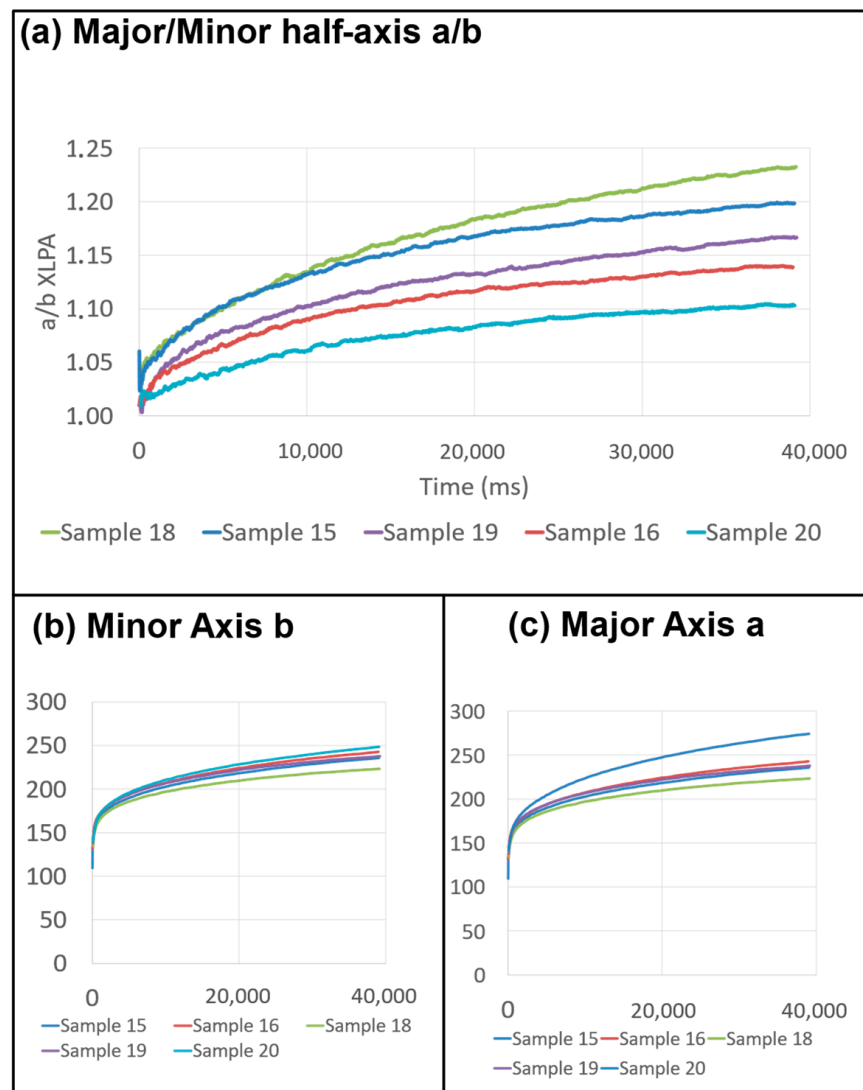


Figure 5. Experimental results of imbibition kinetics obtained from the XLPA device with (a) the anisotropy evaluated in terms of the ratio of the half-axes (a/b), (b) minor axis b , and (c) major axis a . The x -axis represents time in ms.

Based on the results obtained, it can be observed that:

- The same evolution for all the papers. However, the curves differ in their course and position in the coordinate system.
- We recognize a global square root, which corresponds to Lucas–Washburn’s model [27]. For more details about the modeling of such behavior, the interested reader may refer to Bloch et al., 2023 [23], where two regimes are distinguished, namely the initial linear rate then the classical square root shape.
- The imbibition anisotropy (a/b) leads to the following order: 18, 15, 19, 16, 20.
- The minor and major axes lead exactly to the same order (18, 15, 19, 16, 20) from the smaller to the larger values.

The evolution of the main axes depends not only on the fiber orientation but essentially on the porosity.

Indeed, the order of the main axes for the different papers follows the porosity one as presented above.

From the basis weight and thickness, the porosity may be easily calculated. Porosities for papers 18, 15, 19, 16, 20 are 0.561, 0.541, 0.578, 0.573, 0.589, respectively. The results are coherent with the value of the main axis. The results for papers 18 and 20 are clearly

opposite. Papers 16 and 19 behave similarly, as expected. Paper 15 involves a higher jet velocity than the wire. Hence, the formation is not as good/uniform, leading to a behavior similar to paper 19, which is less oriented.

- As the mean pore size is related to the porosity, the evolution of the major axis mainly depends on the porosity, which itself depends on the fiber orientation. The more oriented, the less porous a fibrous structure is. Hence, the time evolution of the imbibition in each main direction should be analyzed based on the porosity.

4. Discussion

It is interesting to compare our results with the ones found in the literature. Fiadero [7] conducted research on the paper anisotropy. We compared their method, based on optical diffraction, to other experimental techniques for precisely the same papers (15–20). We used the same samples as them, called EFGP papers, in their article. The next table is extracted from their article. We added on the last line our results for comparison.

We plot in Figure 6 the anisotropy obtained with different experimental techniques: (a) colorimetric; (b) Lippke; and (c) diffraction vs. the ones obtained with the XLPA imbibition device.

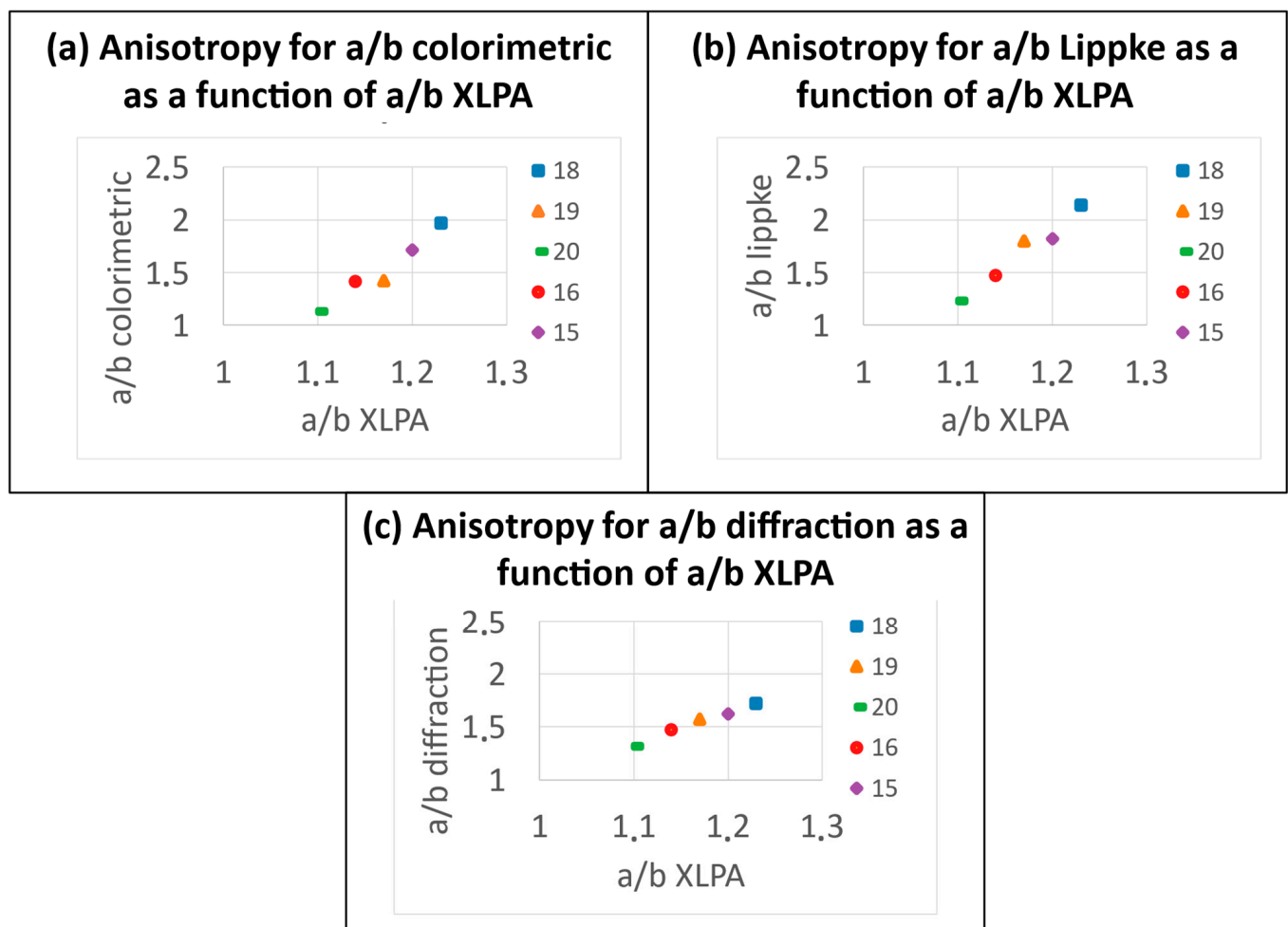


Figure 6. Anisotropy obtained with different experimental techniques (a) colorimetric; (b) Lippke; (c) diffraction vs. imbibition XLPA anisotropy.

Briefly, the colorimetric method is based on the visualization of dyed fibers using transmitted light. The Lippke equipment uses a laser in transmission. The initial round beam is transmitted in an elliptical shape, and its ellipticity is measured. Finally, the

diffraction anisotropy is obtained on a transparent replica of the surface. An optical device based on diffraction is then used to characterize the anisotropy. Here, we do not present a full description of these experimental techniques, as the interested reader may refer to the original article for details.

- Our results fit with all the data presented in Table 2. The anisotropy is well characterized.

Table 2. Anisotropy characterization (ellipticities) for the paper samples (15–20) based on different experimental techniques. All the data are extracted from (Fiadero, 2002) [7], except in the last line, which is obtained from our study with the XLPA device.

Paper	18	19	20	16	15
a/b colorimetric	1.97	1.42	1.13	1.41	1.71
a/b Lippke	2.14	1.8	1.23	1.47	1.82
a/b diffraction	1.72	1.57	1.32	1.47	1.62
TSI (EMD/ECD)	4.53	2.81	1.72	2.39	3.69
a/b XLPA	1.23	1.17	1.1	1.14	1.2

- Furthermore, linear relationships exist between each anisotropy characterization and the one obtained from imbibition. The imbibition anisotropy is, hence, due to fiber orientation.
- The main axes (a, b) of the ellipse are related to porosity, as expected, and therefore to velocities, which are the time derivative of a and b.

To underline the influence of fiber orientation on paper structure, we analyzed the air permeability for all tested samples. Air permeability corresponds to the porosity of the paper. The results are presented in Figure 7.

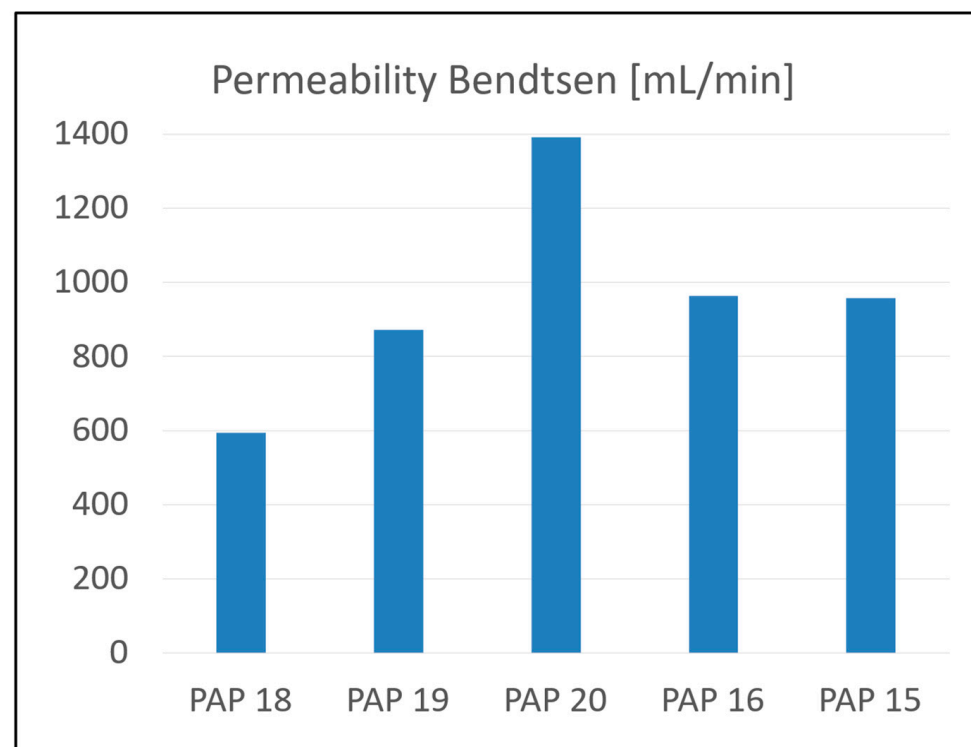


Figure 7. Influence of fiber orientation on Bendtsen permeability for papers 15–20.

The obtained results allow us to conclude that there is a strong dependence between fiber orientation and air permeability. The more isotropic, the higher the permeability.

The effect of fiber orientation for both permanent and transient evolutions, such as imbibition, is therefore highlighted.

5. Conclusions

Based on the research performed, it can be concluded that:

- The main axes representing the main directions of liquid penetration through the paper structure are influenced by the porosity of the fibrous structure.
- Unevenness in the spread of liquid in the tested paper samples was observed during imbibition measurements. It was found that there is a correlation between this effect and anisotropy of paper structure (i.e., differences in fiber orientation).
- The greater the paper anisotropy, the greater the differences in the lengths of the main axes of the ellipse that were observed. A linear dependence is exhibited in our results.
- An experimental device used in the presented research allowed us to characterize the kinetics of imbibition, including small time scales (ms) and larger time (s).

Opportunities for future work consist of studying both the effect of the fluid (using different solvents) to modify the fibers (hardwood, softwood, bleaching) and/or the structures (influence of calendaring, for example).

Author Contributions: P.-Y.B.: Experimentation, investigation, data treatment, and writing; J.-F.B.: theoretical analysis, investigations, data treatment, writing; K.O.: software and hardware, review and editing; D.B.: supervision and review. All authors have read and agreed to the published version of the manuscript.

Funding: This research received no external funding.

Data Availability Statement: The raw data are available on request.

Conflicts of Interest: The authors declare no conflicts of interest.

Appendix A. S1—Experimental Data for Permeability

TESTS	Papers	18	19	20	16	15
Permeability Bendtsen (mL/min)	Rep1	582	802	1327	896	918
	Rep2	524	766	1350	996	912
	Rep3	589	826	1563	922	1080
	Rep4	558	762	1243	997	811
	Rep5	604	739	1692	1095	1077
	Rep6	688	974	1588	905	1253
	Rep7	566	922	1253	984	890
	Rep8	621	874	1480	1028	1043
	Rep9	553	1055	1494	943	732
	Rep10	539	1052	1405	870	1076
	Rep11	636	786	1172	933	924
	Rep12	632	786	1361	938	1097
	Rep13	676	1023	1177	929	837
	Rep14	560	837	1382	1053	749
	Average	595	872	1392	964	957
Std-Dev	50	113	157	64	151	
Coef Var	0.084	0.229	0.113	0.066	0.157	

TESTS	Papers	18	19	20	16	15
Thickness (μm)	Rep1	82	90	85	82	82
	Rep2	82	87	88	79	78
	Rep3	81	89	86	81	77
	Rep4	83	86	90	84	82
	Rep5	84	85	89	83	79
	Rep6	84	82	91	81	84
	Rep7	86	83	94	85	79
	Rep8	84	85	86	79	76
	Rep9	82	85	89	81	80
	Rep10	83	89	87	79	86
	Average	83	86	89	81	80
Std-Dev	1	2	3	2	3	
Coef Var	0.018	0.029	0.031	0.028	0.042	

XLPA raw data are not included in this article but can be provided on request.

References

- Htun, M.; Fellers, C. The In-Plane Anisotropy of Paper in Relation to Fiber Orientation and Drying Restrains. In *Paper Structure and Properties (International Fiber Science and Technology)*; Bristow, J.A., Kolsteh, P., Eds.; CRC Press: Boca Raton, FL, USA, 1986; Volume 327, pp. 327–345.
- Niskanen, K. Paper Structure. In *Paper Physics (Papermaking Science and Technology)*; Tappi Pr: Peachtree Corners, GA, USA, 1998; Volume PST Book 16, pp. 15–51.
- Schaffnit, C.; Silvy, J.; Dodson, C.T.J. Orientation Density Distributions of Fibres in Paper. *Nord. Pulp. Pap. Res. J.* **1992**, *7*, 121–125. [[CrossRef](#)]
- Shakespeare, J. Tutorial: Fibre Orientation Angle Profiles—Process Principles and Cross Machine Control. *TAPPI Process Control Electr. Info. Conf. Proc.* **1998**, *98*, e593–e636.
- Niskanen, K. *Papermaking Science and Technology*; Finnish Paper Engineers' Association: Helsinki, Finland, 2005; Volume 16.
- Yang, C.-F.; Crosby, C.M.; Eusufzai, A.R.K.; Mark, R.E. Determination of Paper Sheet Fiber Orientation Distributions by a Laser Optical Diffraction Method. *J. Appl. Polym. Sci.* **1987**, *34*, 1145–1157. [[CrossRef](#)]
- Fiadeiro, P.T.; Pereira, M.J.T.; Jesus, M.E.P.; Silvy, J.J. The Surface Measurement of Fibre Orientation Anisotropy and Misalignment Angle by Laser Diffraction. *J. Pulp Pap. Sci.* **2002**, *28*, 341–346.
- Dias, P.A.N.; Rodrigues, R.J.; Reis, M.S. Fast Characterization of In-Plane Fiber Orientation at the Surface of Paper Sheets through Image Analysis. *Chemom. Intell. Lab. Syst.* **2023**, *234*, 104761. [[CrossRef](#)]
- Wharen, D.; Haglund, L.; Norman, B. The Power Spectrum of the Basis Weight of Random Sheets. In *Proceedings of the International Paper Physics Conference, Montreal, PQ, Canada, 1971*; pp. 57–59.
- Helbrecht, C.; Langhans, M.; Meckel, T.; Biesalski, M.; Schabel, S. Analyses of the Effects of Fiber Diameter, Fiber Fibrillation, and Fines Content on the Pore Structure and Capillary Flow Using Laboratory Sheets of Regenerated Fibers. *Nord. Pulp. Pap. Res. J.* **2023**, *38*, 425–440. [[CrossRef](#)]
- Ferreira, E.S.; Drummond, J.; Veiga, A.T.V.; Sibellas, A.; Brown, S.; Cranston, E.D.; Martinez, D.M. Mapping Absorbency in Cellulosic Fibres with Iron Tracers. *Carbohydr. Polym.* **2023**, *311*, 120785. [[CrossRef](#)] [[PubMed](#)]
- Olejník, K.; Bloch, J.-F.; Pelczynski, P. Measurement of the Dynamics of Fluid Sorption for Tissue Papers. *Tappi J.* **2019**, *18*, 417–426. [[CrossRef](#)]
- Yang, L.; Liu, J.; Gu, L. Detailed Insights to Liquid Absorption and Liquid-Paper Interaction. In *Proceedings of the XVth Fundamental Research Symposium Cambridge, 2013*; Y' Anson, S.J., Ed.; Fundamental Research Committee (FRC): Manchester, UK, 2013; pp. 585–598.
- Schoelkopf, J.; Matthews, G.P. Influence of Inertia on Liquid Absorption into Paper Coating Structures. *Nord. Pulp. Pap. Res. J.* **2000**, *15*, 422–430. [[CrossRef](#)]
- von Bahr, M.; Kizling, J. Spreading and Penetration of Aqueous Solutions and Water-Borne Inks in Contact with Paper and Model Substrates. In *Advances in Printing Science and Technology*; Pira International: Surrey, UK, 2001; pp. 87–102.
- Liana, D.D.; Raguse, B.; Gooding, J.J.; Chow, E. Recent Advances in Paper-Based Sensors. *Sensors* **2012**, *12*, 11505–11526. [[CrossRef](#)] [[PubMed](#)]

17. Songok, J.; Salminen, P.; Toivakka, M. Temperature Effects on Dynamic Water Absorption into Paper. *J. Colloid Interface Sci.* **2014**, *418*, 373–377. [[CrossRef](#)] [[PubMed](#)]
18. Iglesias, M.C.; Gomez-Maldonado, D.; Via, B.K.; Jiang, Z.; Peresin, M.S. Pulping Processes and Their Effects on Cellulose Fibers and Nanofibrillated Cellulose Properties: A Review. *For. Prod. J.* **2020**, *70*, 10–21. [[CrossRef](#)]
19. Silvy, J. La Transformation Conforme Du Pore Équivalent, Méthode d'homogénéisation de La Texture Des Milieux Polyphasés. *Récents Progrès Génie Procédés Diffus. Lavoisier Tech. Doc.* **1989**, *3*, 506–514.
20. Drouin, B.; Gagnon, R.; Schroder, A.; Butel, M.; Silvy, J. L'Orientation Des Fibres et Les Propriétés Mécaniques Du Papier: Méthodes de Contrôle de l'Anisotropie de La Feuille. *REVUE-ATIP* **1995**, *49*, 66–72.
21. Silvy, J. Etude Structurale Des Milieux Fibreux: Cas Des Fibres Cellulosiques. Ph.D. Thesis, Institut National Polytechnique de Grenoble, Grenoble, France, 1980.
22. Silvy, J.; Caret, C.; Belamaalem, B.; Marhous, M. The Tridimensional Structure of Paper, Methods of Analysis and Implications on His Physical Properties. In *Proceedings of the International Paper Physics Conference; CPPA TAPPI: Niagara on the Lake, ON, Canada, 1995*; pp. 1–5.
23. Bloch, P.-Y.; Olejnik, K.; Bloch, J.-F.; Bloch, A.; Hammond, J.; Brissaud, D. Time Scales of Spontaneous Imbibition into Porous Material: From Classic Models to Papers Applications. *Bioresources* **2023**, *19*, 345–365. [[CrossRef](#)]
24. ISO 5636-3:2013; Paper and Board—Determination of Air Permeance (Medium Range)—Part 3: Bendtsen Method. International Organization for Standardization: Geneva, Switzerland, 2013.
25. ISO 534:2011; Paper and Board—Determination of Thickness, Density and Specific Volume. International Organization for Standardization: Geneva, Switzerland, 2011.
26. Mercer, P. On-Line Instrumentation for Wet-Ended Control. *Appita* **1988**, *41*, 308–312.
27. Hamraoui, A.; Nylander, T. Analytical Approach for the Lucas-Washburn Equation. *J. Colloid Interface Sci.* **2002**, *250*, 415–421. [[CrossRef](#)] [[PubMed](#)]

Disclaimer/Publisher's Note: The statements, opinions and data contained in all publications are solely those of the individual author(s) and contributor(s) and not of MDPI and/or the editor(s). MDPI and/or the editor(s) disclaim responsibility for any injury to people or property resulting from any ideas, methods, instructions or products referred to in the content.